Oecologia
https://doi.org/10.1007/s00442-022-05121-y

PHYSIOLOGICAL ECOLOGY – ORIGINAL RESEARCH

Heterogeneous isotope effects decouple conifer leaf and branch sugar $\delta^{18}O$ and $\delta^{13}C$

Richard P. Fiorella[1,2,6] · Steven A. Kannenberg[3] · William R. L. Anderegg[2,3] · Russell K. Monson[4,5] · James R. Ehleringer[2,3]

Received: 19 April 2021 / Accepted: 21 January 2022

Abstract

Isotope ratios of tree-ring cellulose are a prominent tool to reconstruct paleoclimate and plant responses to environmental variation. Current models for cellulose isotope ratios assume a transfer of the environmental signals recorded in bulk leaf water to carbohydrates and ultimately into stem cellulose. However, the isotopic signal of carbohydrates exported from leaf to branch may deviate from mean leaf values if spatial heterogeneity in isotope ratios exists in the leaf. We tested whether the isotopic heterogeneity previously observed along the length of a ponderosa pine (*Pinus ponderosa*) leaf water was preserved in photosynthetic products. We observed an increase in both sugar and bulk tissue $\delta^{18}O$ values along the needle, but the increase in carbohydrate $\delta^{18}O$ values was dampened relative to the trend observed in leaf water. In contrast, $\delta^{13}C$ values of both sugar and bulk organic matter were invariant along the needle. Phloem-exported sugar measured in the branch below the needles did not match whole-needle values of $\delta^{18}O$ or $\delta^{13}C$. Instead, there was a near-constant offset observed between the branch and needle sugar $\delta^{13}C$ values, while branch $\delta^{18}O$ values were most similar to $\delta^{18}O$ values observed for sugar at the base of the needle. The observed offset between the branch and needle sugar $\delta^{18}O$ values likely arises from partial isotope oxygen exchange between sugars and water during phloem loading and transport. An improved understanding of the conditions producing differential $\delta^{13}C$ and $\delta^{18}O$ isotope effects between branch phloem and needle sugars could improve tree-ring-based climate reconstructions.

Keywords Cellulose · Ponderosa pine · Stable isotopes · Sugars · Tree rings

Introduction

Tree-ring archives have been widely used to reconstruct ecosystem responses to environmental extremes such as drought, and to reconstruct past climate and fire regimes (D'Arrigo et al. 2001; Cook et al. 2010; Babst et al. 2014; Williams et al. 2020). While initial studies on tree-ring archives focused on physical properties of the wood, such as ring widths or density, carbon and oxygen isotope ratios in tree-ring cellulose provide additional process-level information (McCarroll and Loader 2004; Gessler et al. 2014). Tree-ring oxygen isotope ratios have been used to reconstruct climate variables such as temperature, precipitation, or vapor pressure deficit (e.g., Libby et al. 1976; Danis et al. 2006; Treydte et al. 2006; Roden and Ehleringer 2007; Sidorova et al. 2009; Kahmen et al. 2011), while tree-ring carbon isotope ratios have been used to reconstruct variations in intrinsic water use efficiency (e.g., Saurer et al. 2014; Frank et al. 2015; Mathias and Thomas 2021). The wide range of

Communicated by Christiane Roscher.

✉ Richard P. Fiorella
rfiorella@lanl.gov

1 Department of Geology and Geophysics, University of Utah, Salt Lake City, UT 84112, USA

2 Global Change and Sustainability Center, University of Utah, Salt Lake City, UT 84112, USA

3 School of Biological Sciences, University of Utah, Salt Lake City, UT 84112, USA

4 Department of Ecology and Evolutionary Biology, University of Arizona, Tucson, AZ 85721, USA

5 Laboratory of Tree Ring Research, University of Arizona, Tucson, AZ 85721, USA

6 Present Address: Earth and Environmental Sciences Division, Los Alamos National Laboratory, Los Alamos, NM 87545, USA

Published online: 02 February 2022

applications for stable isotope ratios of tree rings has motivated substantial interest in their use, but their utility can be expanded through a more comprehensive knowledge of the environmental factors that drive spatial and temporal variability (Reynolds-Henne et al. 2007; Gessler et al. 2013; Treydte et al. 2014; Cheesman and Cernusak 2016).

Models of tree ring-climate interactions predict how isotope ratios track environmental signals from leaf water to tree-ring cellulose (Farquhar et al. 1989; Saurer et al. 1997; Roden et al. 2000; Barbour and Farquhar 2000; Gessler et al. 2014), with the carbon isotope ratios of C_3 photosynthetic products varying in response to changes in the ratio of the atmosphere-to-leaf CO_2 mole fraction (e.g., Farquhar et al. 1989). Prior studies tracing the isotopic signal of recent photosynthates to tree-ring cellulose have noted that variations in leaf-level $\delta^{13}C$ are often attenuated, perhaps associated with mixing between photosynthates of different ages (Brandes et al. 2006; Gessler et al. 2009; Offermann et al. 2011). Moreover, $\delta^{13}C$ values of sugars exported from the leaves that are used in tree-ring cellulose construction may be offset from their initial values as a result of post-photosynthetic fractionation associated with processes, such as construction and breakdown of transitory starch (Brandes et al. 2006; Gessler et al. 2008), lignin and lipid metabolism (Benner et al. 1987; Hobbie and Werner 2004), respiration and bark photosynthesis (Cernusak and Marshall 2000; Cernusak et al. 2001), and phloem loading and mixing (Offermann et al. 2011; Gessler et al. 2014; Bögelein et al. 2019).

In contrast, the oxygen isotope ratio of leaf sugars is primarily determined by the $\delta^{18}O$ values of the leaf water with an offset of ~ 27‰ (Sternberg et al. 1986; Cernusak et al. 2003; Lehmann et al. 2017). When these sugars are used to build cellulose, a fraction of their oxygen atoms will exchange with the surrounding xylem water. The extent of exchange is thought to be controlled by the fraction of sugars that cycle between hexoses and trioses prior to incorporation into cellulose (Hill et al. 1995; Barbour and Farquhar 2000; Cheesman and Cernusak 2016). These fractionation and exchange processes are commonly modeled using an empirical formula relating to the enrichment of ^{18}O above source water ($\Delta^{18}O_x = (\delta^{18}O_x - \delta^{18}O_{source})/(1 + \delta^{18}O_{source}/1000)$) between leaf water ($\Delta^{18}O_L$) and plant cellulose ($\Delta^{18}O_{cellulose}$) (e.g., Barbour 2007):

$$\Delta^{18}O_{cellulose} = \Delta^{18}O_L\left(1 - p_{ex}p_x\right) + \varepsilon_{wc}$$

where p_{ex} is the fraction of oxygen atoms in sugars that exchange with local water, p_x is the proportion of local water that has not been evaporatively enriched, and ε_{wc} is the oxygen isotope fractionation during cellulose biosynthesis. The $p_{ex}p_x$ term is a 'damping factor,' and reflects the exchange process that prevents full expression of $\Delta^{18}O_L$ variability in cellulose (Cheesman and Cernusak 2016).

An implied assumption in these models is that leaf-exported assimilates reflect the mean $\delta^{18}O$ values measured in leaf water. However, progressive enrichment of heavy water isotopologues–or the tendency of $\delta^{18}O$ to increase along with the leaf and away from veins–has been described many angiosperm and gymnosperm species (Helliker and Ehleringer 2000; Farquhar and Gan 2003; Šantrůček et al. 2007; English et al. 2007), including pines (Shu et al. 2008; Kannenberg et al. 2021). These leaf water isotope ratio heterogeneities may introduce spatial variations into leaf sugar $\delta^{18}O$ values that may not be fully reflected in the phloem.

Within the past decade, several studies have noted that phloem-exported sugars may have $\delta^{18}O$ values lower than expected based on whole-leaf mean isotope ratios (Offermann et al. 2011; Gessler et al. 2013; Treydte et al. 2014). Where this decoupling between leaf and branch isotope ratios occurs, the portion of the tree-ring signal related to leaf-level processes may be attenuated, potentially influencing the interpretation of environmental variation recorded in tree-ring chronologies. This study links water and soluble organic matter in needles, building on the observations of significant needle water ^{18}O enrichment along the length of conifer needles (Kannenberg et al. 2021). We quantified seasonal trends in the concentrations and stable isotope ratios ($\delta^{18}O$ and $\delta^{13}C$) of bulk leaf organic matter, sugar, and α-cellulose along the length of needles of ponderosa pine (*Pinus ponderosa*), an ecologically important and widespread western US conifer that is commonly used in climate reconstructions (Leavitt et al. 2002; Watson and Luckman 2002; Szejner et al. 2016; Martin et al. 2020). We hypothesize that sugar $\delta^{13}C$ values will be homogenous over the leaf (reflecting similar c_i/c_a values), but that sugar $\delta^{18}O$ values will express the progressive enrichment observed in leaf water $\delta^{18}O$. We also hypothesize that cellulose $\delta^{13}C$ and $\delta^{18}O$ values will be homogenous across the leaf, reflecting a common substrate for cellulose synthesis during needle expansion from the base.

Materials and methods

Study site, sample collection and preparation

Samples were collected from five *P. ponderosa* individuals at the base of a southern-aspect slope in Big Cottonwood Canyon, near Salt Lake City, UT (40.6° N, 111.6° W). The mean annual temperature of the site is 5.7 °C, and annual precipitation averages 999 mm (PRISM 1981-2010 climate normals, Daly et al. 2008). Temperature and precipitation at the site are highly seasonal, with mean summer (JJA) temperatures of 16.5°. Moreover, only 10% of annual precipitation falls during JJA, with 67% of annual precipitation falling mostly as snow between November and April.

The most distal sections of three branches were cut from the tree at midday (between 12 and 2 pm local time) on four days during 2019: February 19, June 21, July 23, and September 14. Samples were placed in a cooler containing dry ice until they could be transported back to the lab, where they were kept frozen at − 20 °C until processed further. Needles from the prior year were segmented into thirds lengthwise, microwaved at 700 W for 80 s to inactivate enzymes and oven-dried at 60 °C for two days. A ~ 5 cm-long segment of the branch immediately adjacent to the sampled needles was also microwaved and dried in the same manner as the needles. Sampled branch segments were ~ 2 cm in diameter. After drying, the bark and phloem were separated from the xylem with a razor. Needle and branch bark/phloem samples were ground in a Retsch ball mill for 30 s at 30 Hz.

Leaf and xylem water isotope ratios were collected concurrently in June and September (Kannenberg et al. 2021). Leaf and xylem samples were placed into 20 mL vials and kept on dry ice in a cooler while in the field, and then transferred to a − 20 °C freezer when back at the lab. Xylem samples were collected from the trunk using an increment borer. Water was extracted from leaf and xylem samples using cryogenic distillation until complete; leaf samples were extracted for > 60 min while stem xylem samples were extracted for > 90 min (West et al. 2006). Further details of the water extraction are given in Kannenberg et al. (2021).

Determination of sugar and starch concentrations

Sugar and starch concentrations (% dry weight)—collectively referred to as non-structural carbohydrates (NSC)—were determined colorimetrically (Landhäusser et al. 2018). Sugars were extracted from ground samples in 80% ethanol, oxidized with a phenol–sulfuric acid solution in duplicate, and solution absorbance measured at 490 nm on a Thermo Scientific Genesys20 visible spectrophotometer. Starch was extracted from the remaining solid sample using sequential enzymatic digestion using α-amylase and amyloglucosidase. The supernatant after enzymatic digestion was mixed with perioxidase-glucose oxidase (PGO) reagent in duplicate and sample absorbance measured at 525 nm. More detailed protocols for these methods are found in the supporting information of this article and in Landhäusser et al. (2018).

Cellulose preparation and extraction

Needle segments were ground to a size fraction between 35 and 60 mesh using a mortar and pestle, as the ball mill technique would produce too fine a powder for subsequent extraction. Branch cellulose was obtained by similarly grinding xylem from a section of branch immediately adjacent to the needle samples. For each sample, ~ 250 mg of ground material was loaded into packets made from ANKOM F57 filter bag material (ANKOM Technology; Macedon, NY). Non-cellulosic components were removed from samples sequentially following established methods (Leavitt and Danzer 1993; Loader et al. 1997; Rinne et al. 2005; Boettger et al. 2007). Briefly, sugars and other water-soluble compounds were removed by boiling the sample in deionized water for 1 h, after which the samples were dried at 60 °C overnight. Lipids, resins, and other non-polar compounds were removed using Soxhlet extraction in a 2:1 toluene:ethanol solution for 48 h, and then 95% ethanol for 24 h. After Soxhlet extraction, samples were delignified using an acidified sodium chlorite solution at 70 °C for 2–3 days until samples had turned white. The samples were washed and boiled in deionized water to remove any remaining sodium chlorite and dried at 60 °C overnight. Finally, hemicelluloses were removed by soaking the samples in a 17% sodium hydroxide solution for 1 h and then neutralized by soaking samples in a 10% glacial acetic acid solution for an hour. Samples were dried in a 60 °C oven overnight and weighed upon removal from the sample bags to estimate the cellulose mass fraction.

Determination of isotope ratios in bulk, cellulose, and sugar fractions

Samples for bulk and cellulose fractions were loaded directly into tin (for $\delta^{13}C$) and silver (for $\delta^{18}O$) capsules for isotopic analysis after drying at 60 °C for 48 h. Sugar samples were isolated using a procedure similar to Brugnoli et al. (1988). Roughly 40 mg of bulk needle or phloem material was combined with 1.75 mL of cold (2–8 °C) deionized water and kept at 4 °C for an hour. Samples were centrifuged at 10,700 rpm for 1 min and the supernatant was passed through stacked 5 mL pipette tips containing anionic and cationic exchange resins to remove charged water-soluble compounds that had been co-extracted with the sugars. The upper pipette tip contained DOWEX-50WX8 cation exchange resin (H^+ form, 50–100 mesh), while the lower pipette tip contained DOWEX-1X8 anion exchange resin (Cl^- form, 50–100 mesh). The columns were washed with 8 mL of deionized water to ensure complete elution of dissolved sugars, and all eluted liquid was collected in 15 mL conical tubes. Samples were then frozen and lyophilized and dissolved in 500 µL of deionized water. Small quantities of this solution (10–30 µL) were added to pre-weighed tin (for $\delta^{13}C$) or silver (for $\delta^{18}O$) capsules. Loaded samples were then frozen and lyophilized and the process was repeated until at least 100 µg (300 µg) of material remained in the silver (tin) capsules to ensure sufficient signal.

$\delta^{13}C$ values were determined using EA-IRMS with a Thermo Finnigan Delta Plus XL coupled to a Costech EA 4010 via a Thermo Finnigan ConFlo III. A Zero Blank autosampler from Costech was used to drop individual

samples into the oxidation column. The helium flow rate was set at 90 mL/min. Internal reference materials were two glutamic acids with different carbon isotope ratios and spinach leaves, all calibrated against the USGS40 and USGS41 glutamic acid standards. $\delta^{18}O$ values of solid samples were determined using the glassy-carbon pyrolysis method of Gehre and Strauch (2003) with a high-temperature elemental analyzer (Thermo Finnigan) coupled to a ConFlo III (Thermo Finnigan) referencing interface and a DeltaPlusXL isotope ratio mass spectrometer (TC/EA-IRMS, all supplied by Finnigan MAT; Bremen, Germany). $\delta^{18}O$ values were calibrated to the VSMOW scale using three benzoic acid standards, each having a different oxygen isotope ratio. Measurement precision of quality control standards were < 0.4‰ (SD) for oxygen and < 0.2‰ (SD) for carbon.

Statistical analyses

All data analyses were performed using R, version 4.1.1 (R Core Team 2021). Pairwise differences in mean concentrations or isotope ratios were determined using repeated-measures analysis of variance (ANOVA), with *P* values adjusted for multiple comparisons using the Bonferroni correction. Data were plotted using the ggplot2 package (Wickham 2016).

Results

Bulk isotope ratio patterns

Bulk needle $\delta^{13}C$ and $\delta^{18}O$ values varied over the growing season, but differences along the needle were more pronounced in $\delta^{18}O$ than in $\delta^{13}C$ (Fig. 1). Bulk $\delta^{13}C$ values were greater in February than in June or July in all needle segments ($P < 0.05$, Fig. 1a), except for at the needle tip in July ($P = 0.102$). June and July $\delta^{13}C$ values could not be distinguished in any needle segment. Gradients along the needle in $\delta^{13}C$ values were either not significant or were small. For example, a ~ 1‰ gradient in $\delta^{13}C$ values of bulk tissue was observed in February and June. Basal $\delta^{13}C$ values were higher than those in the middle and tip in February ($P < 0.001$) and were higher in the needle base than the tip in June ($P < 0.002$). No pairwise differences in $\delta^{13}C$ values were observed along the needle in July or September ($P > 0.11$).

In sharp contrast, differences across needle segments in bulk $\delta^{18}O$ values were prominent (Fig. 1b). The bulk $\delta^{18}O$ values of base, middle, and tip segments were statistically distinct at all four measurement periods ($P < 0.0001$, Fig. 1b), with base-to-tip differences ranging from ~ 9‰ (February) to ~ 14‰ (September). At the needle tip, $\delta^{18}O$ values were significantly greater along each progressive measurement period by 1–2‰ ($P < 0.058$, Fig. 1b), while basal $\delta^{18}O$ values varied little in June, July, and September, but were lower than in February ($P < 0.0001$).

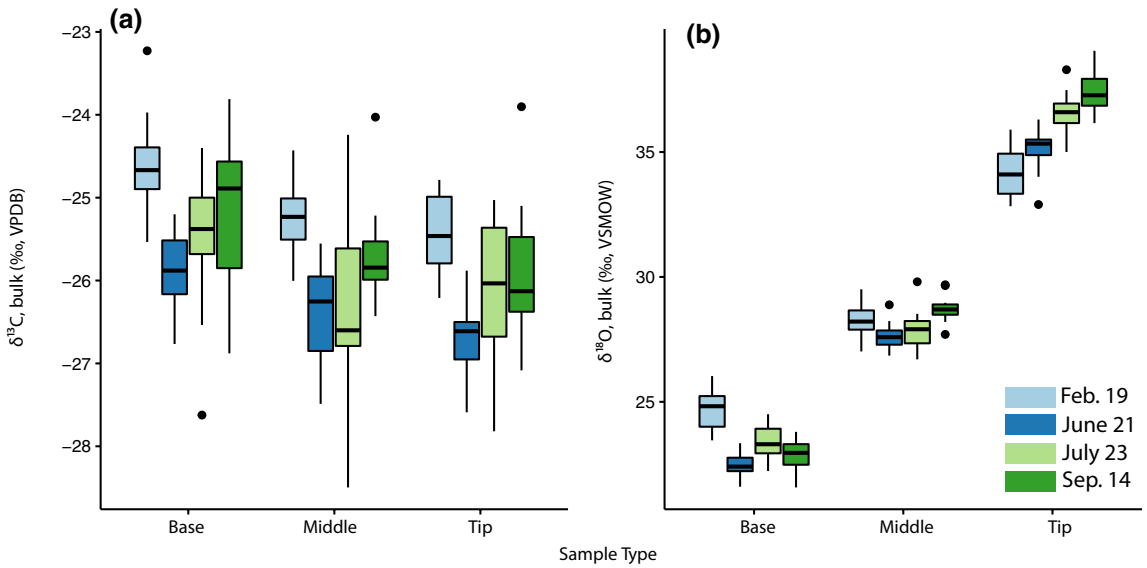

Fig. 1 Boxplots of **a** $\delta^{13}C$ and **b** $\delta^{18}O$ values of bulk organic matter across all needle segments and sampling dates. The horizontal line in each boxplot corresponds to the median isotope ratio, the boxes span the 25th–75th percentiles. Whiskers represent values within 1.5-times of the inter-quartile range (IQR) of the median, and outliers are shown as circles. Boxplot fill colors indicate sampling dates

Seasonal changes in carbohydrate $\delta^{13}C$ and $\delta^{18}O$ values

$\delta^{13}C$ values of needle cellulose were generally higher than sugar $\delta^{13}C$ values (Fig. 2ab), which is consistent with prior studies (e.g., Bowling et al. 2008). Driving the bulk $\delta^{13}C$ variations were changes in median sugar $\delta^{13}C$ values, which were higher in February and September than in June or July (Fig. 2a). Sugar $\delta^{13}C$ values were lower in the branch phloem than in the needle ($P < 0.001$) for all time periods. Along the needle, no significant differences were observed, with the exception that February base $\delta^{13}C$ values were greater than in more distal sections of the needle ($P < 0.003$). Compared to sugar $\delta^{13}C$ values, cellulose $\delta^{13}C$ values exhibited less seasonal variation (Fig. 2b). Along-needle trends in cellulose $\delta^{13}C$ values were observed in February and July cellulose, where $\delta^{13}C$ values were greater than in the needle midsection and tip ($P < 0.03$). No along-needle cellulose $\delta^{13}C$ trends were observed in June and September ($P > 0.12$).

In contrast, sugar $\delta^{18}O$ values consistently exhibited progressive enrichment along the needle (Fig. 2c) as all pairwise sugar $\delta^{18}O$ differences across needle segments were significant ($P < 0.0001$, Fig. 2c). In the basal and middle sections of the needle, sugar $\delta^{18}O$ values were largest in February and September, while at the tip the highest values occurred in July (Fig. 2c). This enrichment trend was strongly dampened in needle cellulose $\delta^{18}O$ values (Fig. 2d), which were all within 5‰ across all sample types and times (Fig. 2d). A small gradient in $\delta^{18}O$ values of 1–2‰ persisted in cellulose, with tip values being larger than middle section values in all months ($P < 0.04$) and larger than basal values in June ($P < 0.0001$) and July ($P = 0.004$). Cellulose $\delta^{18}O$ was higher in the needle than in the branch by ~ 7–10‰ (Fig. 2d).

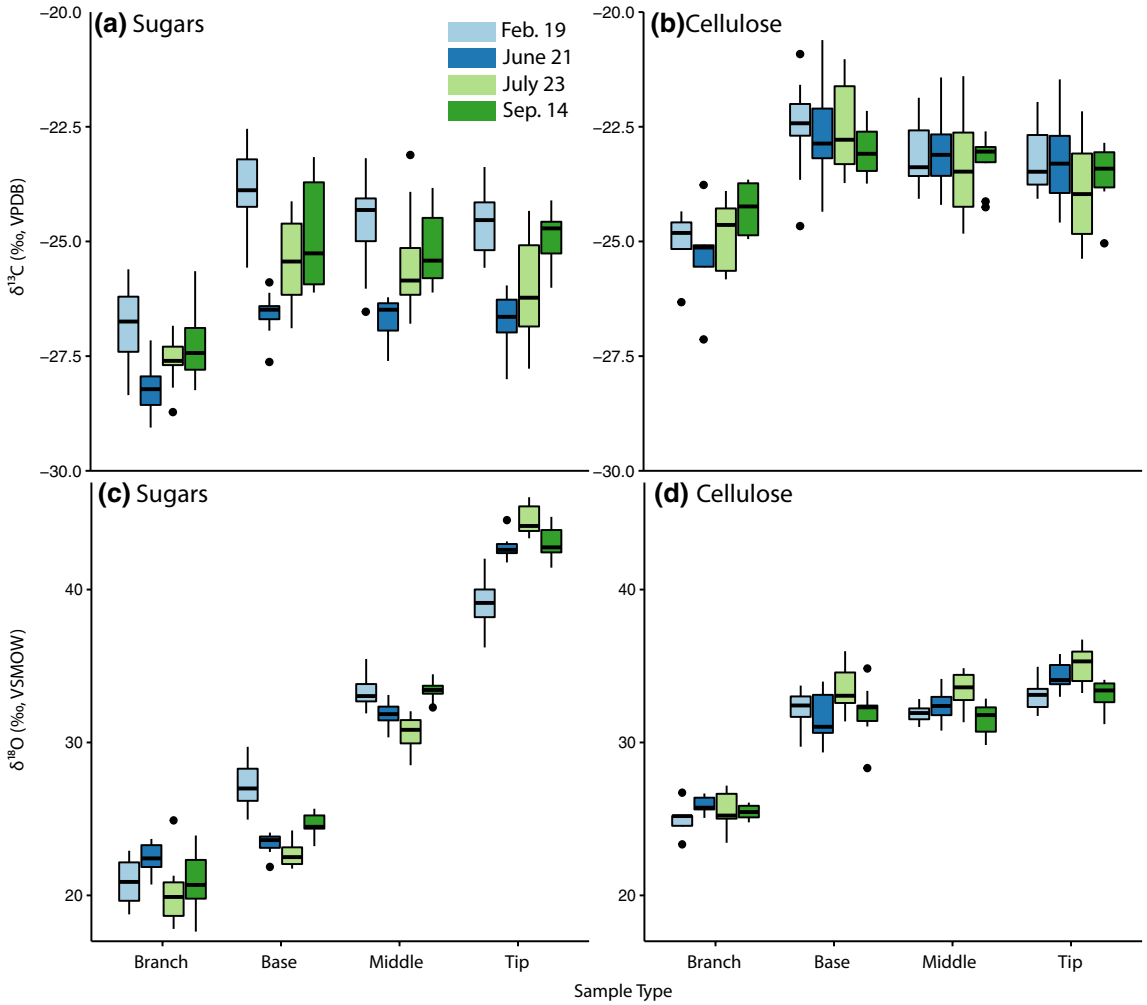

Fig. 2 Boxplots of sugar **a** $\delta^{13}C$ and **b** $\delta^{18}O$ values of in needle segments (base, middle, or tip) and proximal branch phloem, and **c** $\delta^{13}C$ and **d** $\delta^{18}O$ values in needle segment and proximal branch cellulose. The horizontal line in each boxplot corresponds to the median isotope ratio, the boxes span the 25th–75th percentiles. Whiskers represent values within 1.5-times of the IQR of the median, and outliers are shown as circles. Boxplot fill colors indicate sampling dates

Relative to needle sections, sugar $\delta^{18}O$ values in the branch exhibited less variability. Branch sugar $\delta^{18}O$ values were higher in June than in July ($P = 0.02$), but all other pairwise comparisons across time in branch sugar $\delta^{18}O$ values were not significant. All pairwise differences between needle and branch $\delta^{18}O$ values were significant ($P < 0.0007$, Fig. 2c), except between the branch and needle base in June ($P = 0.06$). Progressive enrichment varied by season, from a branch-needle tip difference of ~ 15‰ in February to nearly 25‰ in July.

Seasonal changes in carbohydrate abundances

In addition to changes in component compound isotope ratios, the observed seasonal changes in bulk $\delta^{13}C$ and $\delta^{18}O$ values could have been driven by changes in carbohydrate abundances within a needle. Sugar and starch abundances exhibited opposing trends during the growing season, and seasonal variations in these components were larger than any potential deviations along the needle. Leaf soluble sugar concentrations were higher in February (~ 13% w w^{-1}) than in June and July in all segments (6–10% w w^{-1}, $P < 0.0001$, Fig. 3a). July median sugar concentrations (~ 10–12% w w^{-1}) were greater than June median sugar concentrations (~ 6–8% w w^{-1}), but this difference was not significant ($P > 0.72$). September needle sugar concentrations were lower than in February ($P < 0.01$), but larger than in June ($P < 0.004$, Fig. 3a). In the branch, sugar concentrations were higher in February and September than in June and July ($P < 0.03$); however, February and September values were not significantly different from each other, nor were June or July values ($P = 1.0$). Along the needle, no distinct variations in sugar concentrations were observed ($P > 0.21$). Branch sugar concentrations were lower than in the needle in February ($P < 0.001$) and July ($P < 0.01$), and in the needle middle and tip in September ($P < 0.0003$).

Needle starch concentrations were below the detection limit in February, rose to 5–10% (w w^{-1}) in June, and then decreased to 1–3% (w w^{-1}) for July and September (Fig. 3b). June needle starch concentrations were significantly higher than at all other time periods ($P < 0.001$). February, July, and September needle starch concentrations were not significantly different ($P > 0.06$). Branch starch concentrations were also higher in June than in any other period ($P < 0.001$), and July starch concentrations were higher than February starch concentrations ($P < 0.03$). No significant differences were observed along the needle in starch concentrations ($P > 0.36$), though values were significantly higher than in the branch in September ($P < 0.05$).

The α-cellulose mass fraction was highest in February and June (~ 17% w w^{-1}) before falling to ~ 14–15% in July and ~ 10% in September (Fig. 3c). Needle cellulose percentages in February and June were indistinguishable ($P = 1.0$) but were larger than in September ($P < 0.003$). July needle cellulose percentages were significantly lower than in February and June, and significantly higher than in September at the tip ($P < 0.03$). No significant differences in cellulose fraction along the needle were observed during any collection period ($P > 0.28$).

Relationships between branch and leaf sugar $\Delta^{18}O$ and $\delta^{13}C$ values

A positive but variable correlation was observed between branch and whole-leaf (e.g., averaged across the leaf) sugar $\delta^{13}C$ and $\Delta^{18}O$ values (Fig. 4a, b, Table 1), but no significant relationship between branch sugar $\Delta^{18}O$ and leaf water $\Delta^{18}O$ values was observed (Fig. 4c). Similar relationships were observed when $\delta^{18}O$ values were used instead of $\Delta^{18}O$

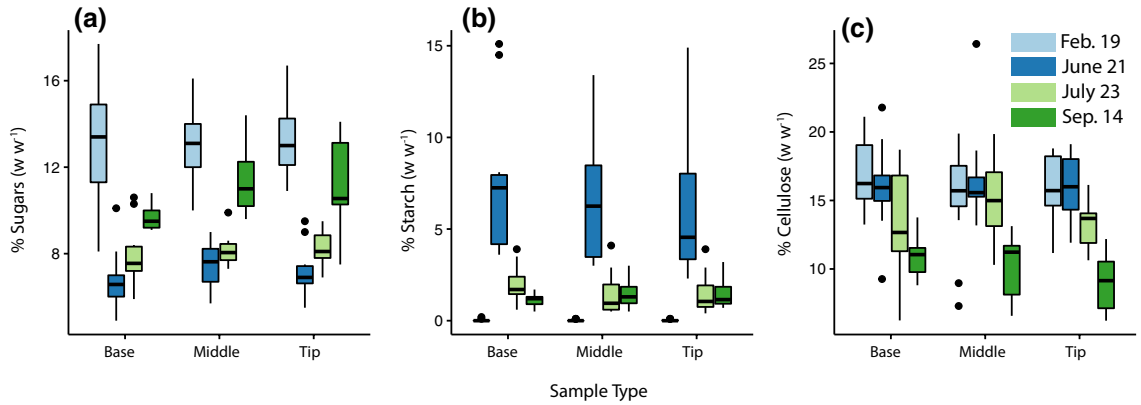

Fig. 3 Percentage of branch and needle segment (base, middle, or tip) dry mass corresponding to **a** soluble sugars, **b** starch, and **c** α-cellulose. The horizontal line in each boxplot corresponds to the median isotope ratio, the boxes span the 25th–75th percentiles. Whiskers represent values within 1.5-times of the IQR of the median, and outliers are shown as circles. Boxplot fill colors indicate sampling dates

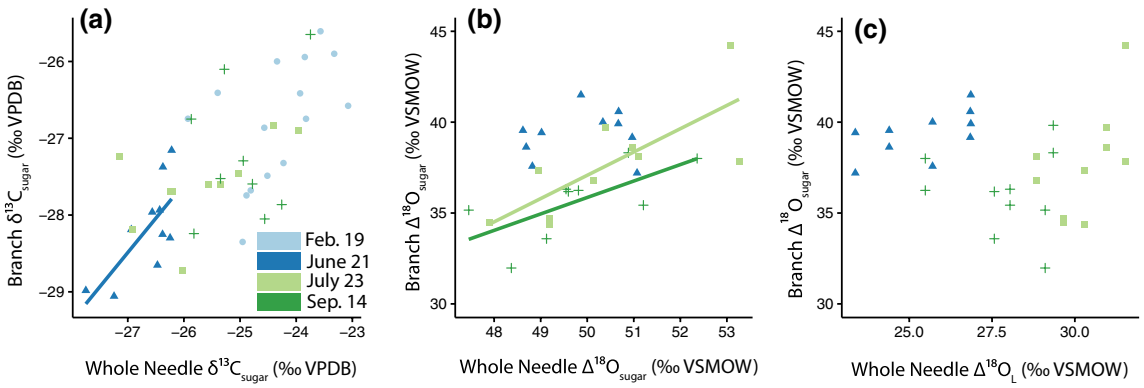

Fig. 4 Relationships between: **a** branch and needle sugar $\delta^{13}C$, and branch sugar $\Delta^{18}O$ with **b** whole-leaf sugar $\Delta^{18}O$ and **c** whole-leaf water $\Delta^{18}O_L$. Best-fit lines are shown when the regressions are significant ($P < 0.05$). February values for $\Delta^{18}O_L$ and $\Delta^{18}O_{sugar}$ were not calculated and are missing from panels **b**, **c**, as no xylem or leaf water samples were collected during this time. Colors and symbols indicate the sampling period (February—light blue circles, June—dark blue triangle, July—light green squares, September—dark green crosses)

Table 1 Seasonal variations in carbon and water isotope ratios between branch and leaf across leaf water and sugars

	Slope	Intercept	*P* value	Correlation
$\delta^{13}C$, branch and whole-leaf sugar				
February	0.49 ± 0.25	− 14.87 ± 6.00	0.068	0.483
June	**0.89 ± 0.31**	**− 4.33 ± 8.20**	**0.020**	**0.717**
July	0.31 ± 0.16	− 19.59 ± 4.09	0.086	0.569
September	0.32 ± 0.46	− 19.26 ± 11.51	0.51	0.253
Pooled—all data	**0.53 ± 0.08**	**− 14.01 ± 2.12**	**< 0.001**	**0.697**
$\Delta^{18}O$, branch sugar and leaf water				
June	0.52 ± 0.26	26.04 ± 6.59	0.078	0.582
September	− 0.09 ± 0.56	38.59 ± 15.53	0.88	− 0.057
Pooled—all data	− 0.12 ± 0.21	41.12 ± 5.74	0.55	− 0.113
$\Delta^{18}O$, branch and whole-leaf sugar				
June	0.15 ± 0.46	31.75 ± 22.90	0.75	0.117
July	**1.28 ± 0.39**	**− 27.01 ± 19.85**	**0.012**	**0.755**
September	**0.91 ± 0.37**	**− 9.40 ± 18.48**	**0.004**	**0.678**
Pooled—all data	**0.95 ± 0.30**	**− 10.00 ± 15.12**	**0.004**	**0.519**
$\Delta^{18}O$, sugar and water in segments				
June	**0.57 ± 0.01**	**34.10 ± 0.44**	**< 0.001**	**0.991**
September	**0.40 ± 0.02**	**37.26 ± 0.65**	**< 0.001**	**0.973**
Pooled—all data	**0.46 ± 0.02**	**36.34 ± 0.57**	**< 0.001**	**0.962**

Regressions significant at the $P = 0.05$ level are printed in bold

values, as xylem water isotope ratios only varied by ~ 2–3‰ throughout the observation period (Kannenberg et al. 2021). Over the season, $\delta^{13}C$ values in-branch sugar were positively correlated with those in the leaf (Fig. 4a, Table 1, $r = 0.694$, $P < 0.001$). The strength of the coupling between the branch and leaf sugar varied throughout our measurements, with the strongest coupling observed in June (Fig. 4a, Table 1, $r = 0.717$, $P = 0.02$). In contrast, the slope of the relationship between branch and whole-leaf sugar $\Delta^{18}O$ values was not significant in June and reached a maximum of 1.28 ± 0.39 in July ($r = 0.755$, $P = 0.012$) before decreasing to 0.91 ± 0.37 in September (Fig. 4b, Table 1, $r = 0.678$, $P = 0.004$). We did not observe any significant correlation between branch sugar $\Delta^{18}O$ and leaf water $\Delta^{18}O$ values in any study period (Fig. 4c, Table 1, $P > 0.07$).

Within needle variations in sugar and leaf water $\Delta^{18}O$

The relationship between midday sugar and leaf water $\Delta^{18}O$ varied across the needle (Fig. 5). Sugar exhibited $\Delta^{18}O$ values ~ 30‰ greater than leaf water $\Delta^{18}O$ values in the basal

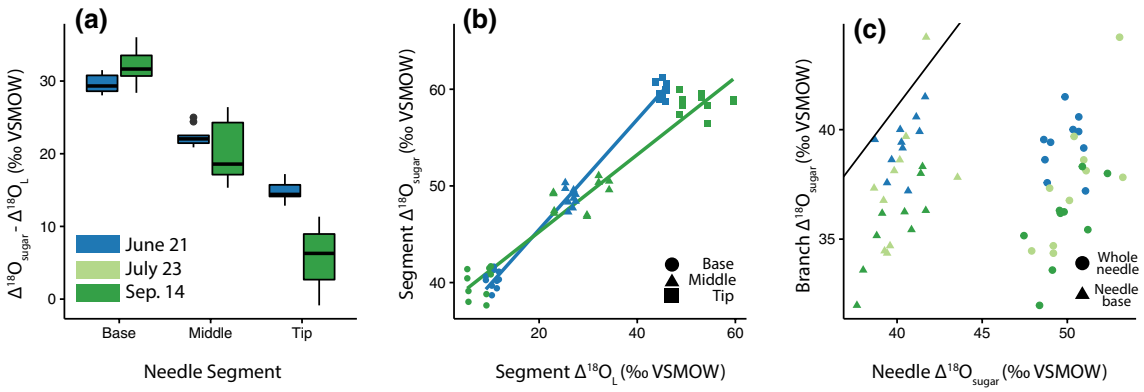

Fig. 5 Relationships between $\Delta^{18}O$ of needle water and sugar: **a** differences between $\Delta^{18}O_{sugar}$ and $\Delta^{18}O_L$ by segment, **b** relationship between $\Delta^{18}O_{sugar}$ and concurrent $\Delta^{18}O_L$ in the same needle segment, and **c** branch and needle $\Delta^{18}O_{sugar}$ in the whole needle (circle) and the basal third only (triangles). The solid black line in panel c) represents the expected equilibrium ^{18}O-enrichment of sugars above leaf water, $\Delta^{18}O_{sugar} = 1.027\Delta^{18}O_L + 27‰$ (e.g., Barbour 2007)

section, decreasing to ~ 18–22‰ in the middle section (Fig. 5a). In the needle tip, sugar $\Delta^{18}O$ values were ~ 15‰ greater than leaf water values during June, but only ~ 7‰ greater on average in September (Fig. 5a). Segment $\Delta^{18}O$ sugar and leaf water values were highly correlated (Fig. 5b), with a regression slope less than one (Table 1). The lower-than-unity slope indicates that midday leaf water enrichment is damped during incorporation into photosynthetic products.

Discussion

Phloem sugar isotope ratios may not reflect whole-needle averages in ponderosa pine

Our results are consistent with previous studies that found evidence that sugars in the phloem had a lower oxygen isotope ratio than observed in leaves (Offermann et al. 2011; Gessler et al. 2013; Treydte et al. 2014). These findings challenge our understanding of the extent to which climatic variations recorded in the $\delta^{18}O$ values of tree-ring cellulose arise from leaf-level water enrichment compared to variations in source water $\delta^{18}O$ values. Gessler et al. (2013) suggested that the offset between phloem and leaf sugar values can be related to oxygen isotope exchange during phloem loading and transport, as well as contributions from sugars fixed by bark photosynthesis (e.g., Cernusak and Marshall 2000) which would have a $\Delta^{18}O$ value of ~ 0‰. Our results suggest that leaf-exported assimilates most closely represent sugar $\delta^{18}O$ values near the needle base in *P. ponderosa* (Fig. 2c), which raises the possibility that sugar may not be equally exported from all portions of the needle, and instead might be biased toward preferential export from the needle base.

Several factors could contribute to the apparent decoupling of phloem sugar $\Delta^{18}O$ from leaf-water isotope ratios, as observed in this study. First, leaf water oxygen isotope ratios are likely to be more dynamic and exhibit greater amplitude in the diel cycle than sugar oxygen isotope ratios (e.g., Cernusak et al. 2005; Barnard et al. 2007; Gessler et al. 2009). As a result, it would be expected that measured sugar $\Delta^{18}O$ values should reflect a dampening of midday leaf water enrichment in our study, since a significant fraction of daily assimilation may have occurred in the morning when $\Delta^{18}O_L$ was lower.

Additionally, our method of extracting sugar from the phloem may promote a further dampening of the leaf-water signal. We chose to extract water-soluble compounds from ground phloem to maintain a consistent extraction method between leaf and phloem and also avoid known issues with phloem sugar extraction (Lehmann et al. 2020). However, this method may have also extracted water-soluble compounds that were not actively transported in the phloem, and therefore isotope ratios may represent a mixture of assimilates of different ages and with different metabolic histories. Notably, $\delta^{13}C$ and $\delta^{18}O$ of sugar alcohols tends to be lower in phloem than in leaves (Rinne et al. 2015; Lehmann et al. 2017). While direct comparisons between phloem and leaf sugar alcohols are sparse, it is likely that their concentration is much higher in leaves (Merchant 2012), which would necessitate an even larger difference between phloem and leaf sugar $\delta^{18}O$ to explain our results.

The temporal signal of leaf-water enrichment recorded by phloem-exported sugars may also be influenced by the diel cycle of transitory starch buildup and breakdown. Chloroplast starch concentrations build during the day and decrease over the night. Hydrolysis of transitory starch may promote oxygen isotope exchange if intermediate products have an exposed carbonyl oxygen, and at a time when $\Delta^{18}O_L$ may

have much lower values than during the day (Barnard et al. 2007; Gessler et al. 2008). As starch concentrations were only measured in midday samples, we cannot quantify the magnitude of the starch diel cycle nor its potential to explain lower sugar values observed in the branch relative to the leaf. However, offsets between the branch and leaf sugar $\Delta^{18}O$ values were larger when starch concentrations were lower (Figs. 2c, 3b, 5c) suggesting that the starch diel cycle is unlikely to contribute significantly to this offset.

Gessler et al. (2013) found that sugar $\Delta^{18}O$ values in the phloem remained lower than in the leaf in two pine species even after accounting for temporal variations in assimilation rates. They concluded that mechanisms related to phloem loading, transport and bark photosynthesis may explain the offset. There is an alternative explanation that could explain both our results and those of Gessler et al. (2013). Sucrose is the dominant sugar transported by phloem and does not contain carbonyl oxygen atoms capable of exchange with those in the surrounding water. However, sucrose has the potential to cycle through successive transformations during transport, breaking down to its monosaccharide constituents–glucose and fructose–followed by reconstitution to a disaccharide. During the monosaccharide phase, up to three of the total 11 oxygen atoms in the sugar molecule may exchange with those in the surrounding water. Since the presence of the Casparian strip within pine needles limits the exchange of water between the xylem and phloem in the center of the needle and the lamina (e.g., Liesche et al. 2011), the water present in the central portion of the needle would likely have a lower $\Delta^{18}O$ value than in the lamina (e.g., Roden et al. 2015). Thus, oxygen isotope exchange could exchange up to 3/11 of the total enrichment signal recorded by sucrose synthesis in the mesophyll if two constraints are met: (a) sucrose is converted to glucose/fructose during or after transport across the Casparian strip, and (b) the water pool interior to the Casparian strip has not experienced evaporative enrichment. In principle, this exchange process can only partially explain the offset between phloem and needle sugar $\Delta^{18}O$ at our site. A leaf $\Delta^{18}O$ sugar value of 50‰ would correspond to a phloem value of 43.7‰, assuming that 3 of 11 oxygen atoms had exchanged in isotopic equilibrium with source water having $\Delta^{18}O = 0$‰.

The observed differences in our study, however, were considerably greater (Figs. 4b, 5c). Moreover, any attenuation of the leaf-water enrichment signal is likely less than the theoretical maximum, because progressive enrichment observed in leaf water $\Delta^{18}O$ requires that water interior to the Casperian strip also exhibit an increase in $\Delta^{18}O$ along the needle (Farquhar and Gan 2003; Shu et al. 2008; Kannenberg et al. 2021). Theoretical models for describing progressive enrichment in $\Delta^{18}O_L$ suggest that the difference between basal $\Delta^{18}O_L$ and whole-leaf average $\Delta^{18}O_L$ should increase with decreasing humidity (Helliker and Ehleringer 2002; Farquhar and Gan 2003; Cernusak et al. 2016), implying that this effect may be particularly acute in arid or semi-arid regions such as our study site.

Phloem transport may also contribute to the attenuation of the leaf-water $\Delta^{18}O$ signal. Transport of sucrose in the phloem is 'leaky,' with a fraction of sucrose lost along the transport pathway (van Bel 2003; De Schepper et al. 2013). Most of the leaked sucrose is reloaded into the phloem, but continuous loss and reloading may result in the mixing of sucrose of different ages, potentially further dampening diel climate signals transferred from leaf water to sugars (Barnard et al. 2007; Gessler et al. 2009, 2014; Treydte et al. 2014). If reloading of the sucrose into the phloem again involves glucose and fructose intermediates, the same three oxygen atoms in the sucrose molecule can exchange again, this time in an environment with an even lower water $\Delta^{18}O$. This process may also entrain sugars produced by bark photosynthesis into the phloem, which would be expected to have oxygen isotope ratios 27‰ above the source water ($\Delta^{18}O = 0$‰) (Sternberg et al. 1986); a value much lower than that expected for leaf assimilates. Stem photosynthesis has been observed in multiple conifer species (Cernusak and Marshall 2000; Berveiller et al. 2007) and appears to be highest in newly grown stems. Our samples were not taken from newly grown branches, but we cannot rule out contributions from stem photosynthesis either from the sampled location in the branch or from newer growth further out on the same branch.

In addition to the mechanisms raised in Gessler et al. (2013), our results raise the possibility that sugars exported from the needle to the branch may be biased toward values at the needle base. Some numerical models have suggested that sugar export from pine needles may be basally biased (Rademaker et al. 2017). However, not all models of phloem transport in pine needles arrive at this conclusion (e.g., Ronellenfitsch et al. 2015). Furthermore, ^{14}C labelling studies have suggested that sugar translocation speed does not vary significantly across the length of individual conifer needles (Han et al. 2019), presenting a further challenge to the idea of basally biased export (Rademaker et al. 2017). Therefore, it seems less likely that offsets between the branch and leaf sugar $\delta^{18}O$ values arise from preferential export of sugars produced at the base of the needle.

Needle cellulose exhibited consistently greater $\delta^{18}O$ values than observed in the adjacent branch, by ~ 7–10‰ (Fig. 2b, d). Curiously, the cellulose $\delta^{18}O$ values were similar to whole-needle sugar $\delta^{18}O$ values (Fig. 2c, d), suggesting that spatial variations in needle $\delta^{18}O$ sugars are homogenized at some point prior to incorporation into needle cellulose. Homogenization is limited, however, as sugar $\delta^{18}O$ values as high as leaf cellulose were never observed in the branch. Alternatively, sugars may undergo additional isotopic exchange with water in the expanding needle, perhaps

during cycling between hexoses and trioses (e.g., Hill et al. 1995). Given that leaf water $\delta^{18}O$ values are enriched relative to water in the xylem, hexose-triose cycling would increase the $\delta^{18}O$ values of sugars being incorporated into needle cellulose. Models of progressive leaf water enrichment suggest that leaf water isotope ratios are more sensitive to atmospheric conditions, and thus more variable, in distal portions of the needle, compared to source water. As a result, water $\delta^{18}O$ values in the vicinity of leaf cellulose biosynthesis near the needle base should be less sensitive to environmental variation, perhaps explaining its near-constant isotope ratio along the needle, since cellulose synthesis and needle expansion occur in the needle base (Kienholz 1934; Campbell 1972; Wright and Leavitt 2006). This finding is consistent with recent studies in grasses that found that the $\delta^{18}O$ in cellulose and $\delta^{2}H$ of *n*-alkanes indicated an isotope ratio of synthesis water that is lower than bulk leaf value (Gamarra et al. 2016; Lehmann et al. 2017). In addition, cellulose and sugar $\delta^{18}O$ values may be reflecting different time periods. For example, substrates used to construct needle cellulose may have been assimilated during the previous growing season.

Carbon isotope ratio differences from branch to needles

Branch sugar $\delta^{13}C$ values were consistently ~ 2–3‰ lower than in the leaf (Fig. 2a). Since no trend in $\delta^{13}C$ values was observed along the needle, this pattern suggests there is an apparent isotopic fractionation process associated with sugars between the needle and the branch. Prior studies investigating $\delta^{13}C$ values in leaves and the nearby phloem have also noted this trend (Gessler et al. 2013, 2014). The observed fractionation has been attributed to post-photosynthetic metabolism, such as during lignin and lipid biosynthesis (e.g., Hobbie and Werner 2004), synthesis and hydrolysis of transitory starch (e.g., Brandes et al. 2006), differences in respiratory fractionation, bark photosynthesis (Cernusak et al. 2009), or compartmentalization and/or mixing of different carbon pools (e.g., Bögelein et al. 2019). Our results do not clarify this issue.

Needle cellulose exhibited consistently higher $\delta^{13}C$ values than observed in the adjacent branch, by ~ 1–3‰ (Fig. 2bd). The ~ 1–3‰ offset in $\delta^{13}C$ values observed between branch and needle cellulose was comparable to the difference between branch and needle sugar $\delta^{13}C$ values (Fig. 2a). Since the carbon source for constructing new needle cellulose is thought to be derived from carbon stored in prior years' needles (Kozlowski 1964; Dickmann and Kozlowski 1968), this pattern suggests that the apparent carbon isotope fractionation associated with the transport of sugars from the needle to the phloem also occurs as sugars are transported into a growing needle. However, a similar pattern would be expected if the expanding needle produced the sugars used to construct cellulose within the same needle; our data cannot distinguish between these possibilities. Moreover, the slight trend observed in cellulose $\delta^{13}C$ values along the needle suggests could also arise from either or both of these processes.

Implications for interpretations of tree-ring isotope ratios

Oxygen isotope ratios of tree-ring cellulose are often interpreted to reflect both the plant's source water and climatic conditions via their influence on leaf-level processes (e.g., McCarroll and Loader 2004; Reynolds-Henne et al. 2007; Treydte et al. 2007; Saurer et al. 2012; Vitali et al. 2021). Our data, consistent with several other studies (Treydte et al. 2014; Gessler et al. 2014; Cheesman and Cernusak 2016; Miranda et al. 2021), suggest the ways through which the leaf-water signal is ultimately recorded in wood cellulose may be more complicated than expressed in current models. While Treydte et al. (2014) found reliable relationships between climate variations and tree-ring cellulose $\delta^{18}O$, they noted that such relations should be strongest in humid regions with precipitation maxima during the growing season. Miranda et al. (2021) reported general consistency with model predictions in trends between climate variation and tree-ring cellulose $\delta^{18}O$ and $\delta^{13}C$ along a sharp altitudinal gradient in the Canary Islands, even at the least humid sites. Other studies, however, have shown that while general trends in cellulose isotope values follow large environmental gradients, the process-based modeling of isotope values through the component chains from leaf water pools through sucrose to cellulose are not easily resolved (Schmidt et al. 2001; Lehmann et al. 2017). Modeling is likely to be confounded by species- and tissue-specific dynamics and post-assimilation processes, as well as unique dependencies on the atmospheric environment. Our results highlight the importance of resolving how within-needle fractionation gradients transfer from leaf water pools to the tree-ring record.

Progressive leaf-water enrichment models suggest that the leaf water environment varies weakly with atmospheric conditions at the base of the leaf and that leaf water $\delta^{18}O$ values are far more sensitive to atmospheric changes at the leaf tip (Farquhar and Gan 2003; Shu et al. 2008; Kannenberg et al. 2021). We suspect that the decoupling between whole-leaf and phloem sugar $\delta^{18}O$ is most significant in arid conditions, as these conditions promote the largest-magnitude of base-to-tip water $\delta^{18}O$ heterogeneities (Helliker and Ehleringer 2002; Farquhar and Gan 2003; Shu et al. 2008; Kannenberg et al. 2021). An additional damping of the leaf water signal was reported in the Barbour and Farquhar (2000) model relating leaf-water isotope ratios to tree-ring cellulose and can be accounted for by

allowing the p_{ex} parameter to vary. However, our results and the results of prior studies (Offermann et al. 2011; Gessler et al. 2013; Treydte et al. 2014) caution that these apparent variations in p_{ex} may not solely reflect variations in the degree of hexose-triose cycling, and that multiple physiological processes may instead be responsible.

Conclusions

Models of tree-ring cellulose isotope ratios often rely on predictions of whole-leaf water isotope ratios. However, spatial heterogeneity in leaf water isotope ratios is common and could bias these relationships if exported sugars do not reflect whole-leaf values. In our study of ponderosa pine, we found that branch $\delta^{13}C$ and $\delta^{18}O$ values in exported sugars were distinct from whole-needle values. Offsets in sugar $\delta^{13}C$ values were fixed and did not vary with position in the leaf, but a small along-needle trend was observed in cellulose. This effect most likely reflects the mixing of multiple carbon pools or effects of post-photosynthetic metabolism (Hobbie and Werner 2004; Brandes et al. 2006; Bögelein et al. 2019), and perhaps variations in environmental conditions during needle expansion (Wright and Leavitt, 2006). In contrast, needle sugar $\delta^{18}O$ values expressed a progressive enrichment in $\delta^{18}O$ from base to tip. We conclude that the origin of this gradient in needle sugar $\delta^{18}O$ arises from the progressive increase in leaf water $\delta^{18}O$ during initial sugar synthesis. The $\delta^{18}O$ of sugars exported from the leaf do not appear to reflect whole-leaf averages and instead are most similar to sugars at the needle base, in contrast to commonly applied cellulose isotope models. This offset between branch and needle likely arises from oxygen isotope exchange during phloem loading and transport, and may be further augmented in the branch by contributions from stem photosynthesis. The presence of oxygen isotope ratio gradients in leaf sugars, and the apparent lack of these gradients in conifer needle cellulose, presents a new opportunity for tracing isotope ratio signals from sugars to their incorporation in sink tissues and improving cellulose isotope ratio models.

Supplementary Information The online version contains supplementary material available at https://doi.org/10.1007/s00442-022-05121-y.

Acknowledgements We thank Avery W. Driscoll and Nic Bitter for field assistance, and Hayley G. Lind, Sierra Hymas, and Suvankar Chakraborty for laboratory assistance.

Author contribution statement All authors contributed to the planning and design of the research, contributed to the interpretation of the data, and wrote the manuscript. RPF and SAK conducted fieldwork and collected the samples, RPF performed the sample preparation and analysis and wrote the initial draft of the manuscript.

Funding RPF, SAK, WRLA, and JRE were supported by the National Science Foundation (NSF) under Grant number 1753845; RKM was supported by NSF Grant number 1754430. RPF and WRLA also received support from NSF Grant number 1802880. RPF also acknowledges support from NSF Grant number 1954660 and WRLA acknowledges support from the David and Lucille Packard Foundation, NSF Grant number 1714972, and the United States Department of Agriculture under Grant number 2018–67019-27850.

Data availability The isotope ratio and chemical abundance data that support the findings of this study are openly available in figshare at http://doi.org/10.6084/m9.figshare.13394870. Climatological data are available from the PRISM (Parameter-elevation Regressions on Independent Slopes Model) Climate Group as part of the Norm81m data product at prism.oregonstate.edu.

Declarations

Conflicts of interest The authors declare that they have no conflicts of interest.

References

Babst F, Alexander MR, Szejner P, Bouriaud O, Klesse S, Roden J et al (2014) A tree-ring perspective on the terrestrial carbon cycle. Oecologia 176:307–322. https://doi.org/10.1007/s00442-014-3031-6

Barbour MM (2007) Stable oxygen isotope composition of plant tissue: a review. Funct Plant Biol 34:83. https://doi.org/10.1071/FP06228

Barbour MM, Farquhar GD (2000) Relative humidity- and ABA-induced variation in carbon and oxygen isotope ratios of cotton leaves. Plant Cell Environ 23:473–485. https://doi.org/10.1046/j.1365-3040.2000.00575.x

Barnard RL, Salmon Y, Kodama N, Sörgel K, Holst J, Rennenberg H et al (2007) Evaporative enrichment and time lags between $\delta^{18}O$ of leaf water and organic pools in a pine stand. Plant Cell Environ 30:539–550. https://doi.org/10.1111/j.1365-3040.2007.01654.x

Benner R, Fogel ML, Sprague EK, Hodson RE (1987) Depletion of ^{13}C in lignin and its implications for stable carbon isotope studies. Nature 329:708–710. https://doi.org/10.1038/329708a0

Berveiller D, Kierzkowski D, Damesin C (2007) Interspecific variability of stem photosynthesis among tree species. Tree Physiol 27:53–61. https://doi.org/10.1093/treephys/27.1.53

Boettger T, Haupt M, Knöller K, Weise SM, Waterhouse JS, Rinne KT et al (2007) Wood cellulose preparation methods and mass spectrometric analyses of $\delta^{13}C$, $\delta^{18}O$, and nonexchangeable $\delta^{2}H$ values in cellulose, sugar, and starch: an interlaboratory comparison. Anal Chem 79:4603–4612. https://doi.org/10.1021/ac0700023

Bögelein R, Lehmann MM, Thomas FM (2019) Differences in carbon isotope leaf-to-phloem fractionation and mixing patterns along a vertical gradient in mature European beech and Douglas fir. New Phytol. https://doi.org/10.1111/nph.15735

Bowling DR, Pataki DE, Randerson JT (2008) Carbon isotopes in terrestrial ecosystem pools and CO_2 fluxes. New Phytol 178:24–40. https://doi.org/10.1111/j.1469-8137.2007.02342.x

Brandes E, Kodama N, Whittaker K, Weston C, Rennenberg H, Keitel C et al (2006) Short-term variation in the isotopic composition of organic matter allocated from the leaves to the stem of Pinus sylvestris: effects of photosynthetic and postphotosynthetic

carbon isotope fractionation. Glob Change Biol 12:1922–1939. https://doi.org/10.1111/j.1365-2486.2006.01205.x
Brugnoli E, Hubick KT, von Caemmerer S, Wong SC, Farquhar GD (1988) Correlation between the carbon isotope discrimination in leaf starch and sugars of C3 plants and the ratio of intercellular and atmospheric partial pressures of carbon dioxide. Plant Physiol 88:1418–1424. https://doi.org/10.1104/pp.88.4.1418
Campbell R (1972) Electron microscopy of the development of needles of Pinus nigra var. maritima. Ann Bot 36:711–720. https://doi.org/10.1093/oxfordjournals.aob.a084627
Cernusak LA, Marshall JD (2000) Photosynthetic refixation in branches of Western White Pine. Funct Ecol 14:300–311. https://doi.org/10.1046/j.1365-2435.2000.00436.x
Cernusak LA, Marshall JD, Comstock JP, Balster NJ (2001) Carbon isotope discrimination in photosynthetic bark. Oecologia 128:24–35. https://doi.org/10.1007/s004420100629
Cernusak LA, Wong SC, Farquhar GD (2003) Oxygen isotope composition of phloem sap in relation to leaf water in Ricinus communis. Funct Plant Biol 30:1059. https://doi.org/10.1071/FP03137
Cernusak LA, Farquhar GD, Pate JS (2005) Environmental and physiological controls over oxygen and carbon isotope composition of Tasmanian blue gum, Eucalyptus globulus. Tree Physiol 25:129–146. https://doi.org/10.1093/treephys/25.2.129
Cernusak LA, Tcherkez G, Keitel C, Cornwell WK, Santiago LS, Knohl A et al (2009) Why are non-photosynthetic tissues generally 13C enriched compared with leaves in C3 plants? Review and synthesis of current hypotheses. Funct Plant Biol 36:199. https://doi.org/10.1071/FP08216
Cernusak LA, Barbour MM, Arndt SK, Cheesman AW, English NB, Field TS et al (2016) Stable isotopes in leaf water of terrestrial plants. Plant Cell Environ 39:1087–1102. https://doi.org/10.1111/pce.12703
Cheesman AW, Cernusak LA (2016) Infidelity in the outback: climate signal recorded in $\Delta^{18}O$ of leaf but not branch cellulose of eucalypts across an Australian aridity gradient. Tree Physiol. https://doi.org/10.1093/treephys/tpw121
Cook ER, Anchukaitis KJ, Buckley BM, D'Arrigo RD, Jacoby GC, Wright WE (2010) Asian monsoon failure and megadrought during the last millennium. Science 328:486–489. https://doi.org/10.1126/science.1185188
D'Arrigo R, Villalba R, Wiles G (2001) Tree-ring estimates of Pacific decadal climate variability. Clim Dyn 18:219–224
Daly C, Halbleib M, Smith JI, Gibson WP, Doggett MK, Taylor GH et al (2008) Physiographically sensitive mapping of climatological temperature and precipitation across the conterminous United States. Int J Climatol 28:2031–2064
Danis PA, Masson-Delmotte V, Stievenard M, Guillemin MT, Daux V, Naveau P et al (2006) Reconstruction of past precipitation $\delta^{18}O$ using tree-ring cellulose $\delta^{18}O$ and $\delta^{13}C$: A calibration study near Lac d'Annecy, France. Earth Planet Sci Lett 243:439–448. https://doi.org/10.1016/j.epsl.2006.01.023
De Schepper V, De Swaef T, Bauweraerts I, Steppe K (2013) Phloem transport: a review of mechanisms and controls. J Exp Bot 64:4839–4850. https://doi.org/10.1093/jxb/ert302
Dickmann DI, Kozlowski TT (1968) Mobilization by Pinus resinosa cones and shoots of C14-photosynthate from needles of different ages. Am J Bot 55:900–906
English NB, Dettman DL, Sandquist DR, Williams DG (2007) Past climate changes and ecophysiological responses recorded in the isotope ratios of saguaro cactus spines. Oecologia 154:247–258. https://doi.org/10.1007/s00442-007-0832-x
Farquhar GD, Gan KS (2003) On the progressive enrichment of the oxygen isotopic composition of water along a leaf: Leaf water isotope modelling. Plant Cell Environ 26:1579–1597. https://doi.org/10.1046/j.0016-8025.2001.00829.x-i1
Farquhar GD, Ehleringer JR, Hubick KT (1989) Carbon isotope discrimination and photosynthesis. Annu Rev Plant Physiol Plant Mol Biol 40:503–537
Frank DC, Poulter B, Saurer M, Esper J, Huntingford C, Helle G, Treydte K et al (2015) Water-use efficiency and transpiration across European forests during the Anthropocene. Nat Clim Change 5:579–583. https://doi.org/10.1038/nclimate2614
Gamarra B, Sachse D, Kahmen A (2016) Effects of leaf water evaporative ^{2}H-enrichment and biosynthetic fractionation on leaf wax *n*-alkane $\delta^{2}H$ values in C3 and C4 grasses. Plant Cell Environ 39:2390–2403. https://doi.org/10.1111/pce.12789
Gehre M, Strauch G (2003) High-temperature elemental analysis and pyrolysis techniques for stable isotope analysis. Rapid Commun Mass Spectrom 17:1497–1503. https://doi.org/10.1002/rcm.1076
Gessler A, Tcherkez G, Peuke AD, Ghashghaie J, Farquhar GD (2008) Experimental evidence for diel variations of the carbon isotope composition in leaf, stem and phloem sap organic matter in Ricinus communis. Plant Cell Environ 31:941–953. https://doi.org/10.1111/j.1365-3040.2008.01806.x
Gessler A, Brandes E, Buchmann N, Helle G, Rennenberg H, Barnard RL (2009) Tracing carbon and oxygen isotope signals from newly assimilated sugars in the leaves to the tree-ring archive. Plant Cell Environ 32:780–795. https://doi.org/10.1111/j.1365-3040.2009.01957.x
Gessler A, Brandes E, Keitel C, Boda S, Kayler ZE, Granier A et al (2013) The oxygen isotope enrichment of leaf-exported assimilates - does it always reflect lamina leaf water enrichment? New Phytol 200:144–157. https://doi.org/10.1111/nph.12359
Gessler A, Ferrio JP, Hommel R, Treydte K, Werner RA, Monson RK (2014) Stable isotopes in tree rings: towards a mechanistic understanding of isotope fractionation and mixing processes from the leaves to the wood. Tree Physiol 34:796–818. https://doi.org/10.1093/treephys/tpu040
Han X, Turgeon R, Schulz A, Liesche J (2019) Environmental conditions, not sugar export efficiency, limit the length of conifer leaves. Tree Physiol 39:312–319. https://doi.org/10.1093/treephys/tpy056
Helliker BR, Ehleringer JR (2000) Establishing a grassland signature in veins: ^{18}O in the leaf water of C3 and C4 grasses. Proc Natl Acad Sci 97:7894–7898. https://doi.org/10.1073/pnas.97.14.7894
Helliker BR, Ehleringer JR (2002) Differential ^{18}O enrichment of leaf cellulose in C3 versus C4 grasses. Funct Plant Biol 29:435. https://doi.org/10.1071/PP01122
Hill SA, Waterhouse JS, Field EM, Switsur VR, Ap Rees T (1995) Rapid recycling of triose phosphates in oak stem tissue. Plant Cell Environ 18:931–936. https://doi.org/10.1111/j.1365-3040.1995.tb00603.x
Hobbie EA, Werner RA (2004) Intramolecular, compound-specific, and bulk carbon isotope patterns in C_3 and C_4 plants: a review and synthesis. New Phytol 161:371–385. https://doi.org/10.1111/j.1469-8137.2004.00970.x
Kahmen A, Sachse D, Arndt SK, Tu KP, Farrington H, Vitousek PM et al (2011) Cellulose $\delta^{18}O$ is an index of leaf-to-air vapor pressure difference (VPD) in tropical plants. Proc Natl Acad Sci 108:1981–1986. https://doi.org/10.1073/pnas.1018906108
Kannenberg SA, Fiorella RP, Anderegg WRL, Monson RK, Ehleringer JR (2021) Seasonal and diurnal trends in progressive isotope enrichment along needles in two pine species. Plant Cell Environ 44:143–155. https://doi.org/10.1111/pce.13915
Kienholz R (1934) Leader, needle, cambial, and root growth of certain conifers and their interrelations. Bot Gaz 96:73–92. https://doi.org/10.1086/334447
Kozlowski TT (1964) Shoot growth in woody plants. Bot Rev 30:335–392. https://doi.org/10.1007/BF02858538
Landhäusser SM, Chow PS, Dickman LT, Furze ME, Kuhlman I, Schmid S et al (2018) Standardized protocols and procedures can precisely and accurately quantify non-structural

carbohydrates. Tree Physiol 38:1764–1778. https://doi.org/10.1093/treephys/tpy118
Leavitt SW, Danzer SR (1993) Method for batch processing small wood samples to holocellulose for stable-carbon isotope analysis. Anal Chem 65:87–89. https://doi.org/10.1021/ac00049a017
Leavitt SW, Wright WE, Long A (2002) Spatial expression of ENSO, drought, and summer monsoon in seasonal $\delta^{13}C$ of ponderosa pine tree rings in southern Arizona and New Mexico. J Geophys Res 107:4349. https://doi.org/10.1029/2001JD001312
Lehmann MM, Gamarra B, Kahmen A, Siegwolf RTW, Saurer M (2017) Oxygen isotope fractionations across individual leaf carbohydrates in grass and tree species: $\delta^{18}O$ of individual leaf carbohydrates. Plant Cell Environ 40:1658–1670. https://doi.org/10.1111/pce.12974
Lehmann MM, Goldsmith GR, Mirande-Ney C, Weigt RB, Schönbeck L, Kahmen A et al (2020) The ^{18}O-signal transfer from water vapour to leaf water and assimilates varies among plant species and growth forms. Plant Cell Environ 43:510–523. https://doi.org/10.1111/pce.13682
Libby LM, Pandolfi LJ, Payton PH, Marshall J, Becker B, Giertz-Sienbenlist V (1976) Isotopic tree thermometers. Nature 261:284–288. https://doi.org/10.1038/261284a0
Liesche J, Martens HJ, Schulz A (2011) Symplasmic transport and phloem loading in gymnosperm leaves. Protoplasma 248:181–190. https://doi.org/10.1007/s00709-010-0239-0
Loader NJ, Robertson I, Barker AC, Switsur VR, Waterhouse JS (1997) An improved technique for the batch processing of small wholewood samples to alpha cellulose. Chem Geol 136:313–317
Martin JT, Pederson GT, Woodhouse CA, Cook ER, McCabe G, Anchukaitis KJ et al (2020) Increased drought severity tracks warming in the United States' largest river basin. Proc Natl Acad Sci 117:11328–11336. https://doi.org/10.1073/pnas.1916208117
Mathias JM, Thomas RB (2021) Global tree intrinsic water use efficiency is enhanced by increased atmospheric CO_2 and modulated by climate and plant functional types. Proc Natl Acad Sci 118:e2014286118. https://doi.org/10.1073/pnas.2014286118
McCarroll D, Loader NJ (2004) Stable isotopes in tree rings. Quat Sci Rev 23:771–801. https://doi.org/10.1016/j.quascirev.2003.06.017
Merchant A (2012) Developing phloem $\delta^{13}C$ and sugar composition as indicators of water deficit in Lupinus angustifolius. HortScience 47:6. https://doi.org/10.21273/HORTSCI.47.6.691
Miranda JC, Lehmann MM, Saurer M, Altman J, Treydte K (2021) Insight into Canary Island pine physiology provided by stable isotope patterns of water and plant tissues along an altitudinal gradient. Tree Physiol 00:1–16. https://doi.org/10.1093/treephys/tpab046
Offermann C, Ferrio JP, Holst J, Grote R, Siegwolf R, Kayler Z et al (2011) The long way down–are carbon and oxygen isotope signals in the tree ring uncoupled from canopy physiological processes? Tree Physiol 31:1088–1102. https://doi.org/10.1093/treephys/tpr093
R Core Team (2021) R: A Language and Environment for Statistical Computing. R Foundation for Statistical Computing, Vienna
Rademaker H, Zwieniecki MA, Bohr T, Jensen KH (2017) Sugar export limits size of conifer needles. Phys Rev E 95:042402. https://doi.org/10.1103/PhysRevE.95.042402
Reynolds-Henne CE, Siegwolf RTW, Treydte KS, Esper J, Henne S, Saurer M (2007) Temporal stability of climate-isotope relationships in tree rings of oak and pine (Ticino, Switzerland). Glob Biogeochem Cycles 21:4009. https://doi.org/10.1029/2007GB002945
Rinne KT, Boettger T, Loader NJ, Robertson I, Switsur VR, Waterhouse JS (2005) On the purification of α-cellulose from resinous wood for stable isotope (H, C and O) analysis. Chem Geol 222:75–82. https://doi.org/10.1016/j.chemgeo.2005.06.010
Rinne KT, Saurer M, Kirdyanov AV, Bruyukhanova MV, Prokushkin AS et al (2015) Examining the response of needle carbohydrates from Siberian larch trees to climate using compound-specific $\delta^{13}C$ and concentration analyses. Plant Cell Environ 38:2340–2352. https://doi.org/10.1111/pce.12554
Roden JS, Ehleringer JR (2007) Summer precipitation influences the stable oxygen and carbon isotopic composition of tree-ring cellulose in Pinus ponderosa. Tree Physiol 27:491–501. https://doi.org/10.1093/treephys/27.4.491
Roden JS, Lin G, Ehleringer JR (2000) A mechanistic model for interpretation of hydrogen and oxygen isotope ratios in tree-ring cellulose. Geochim Cosmochim Acta 64:21–35. https://doi.org/10.1016/S0016-7037(99)00195-7
Roden J, Kahmen A, Buchmann N, Siegwolf R (2015) The enigma of effective path length for ^{18}O enrichment in leaf water of conifers. Plant Cell Environ 38:2551–2565. https://doi.org/10.1111/pce.12568
Ronellenfitsch H, Liesche J, Jensen KH, Holbrook NM, Schulz A, Katifori E (2015) Scaling of phloem structure and optimality of photoassimilate transport in conifer needles. Proc R Soc B Biol Sci 282:20141863. https://doi.org/10.1098/rspb.2014.1863
Šantrůček J, Květoň J, Šetlík J, Bulíčková L (2007) Spatial variation of deuterium enrichment in bulk water of snowgum leaves. Plant Physiol 143:88–97. https://doi.org/10.1104/pp.106.089284
Saurer M, Aellen K, Siegwolf R (1997) Correlating $\delta^{13}C$ and $\delta^{18}O$ in cellulose of trees. Plant Cell Environ 20:1543–1550
Saurer M, Kress A, Leuenberger M, Rinne KT, Treydte KS, Siegwolf RTW (2012) Influence of atmospheric circulation patterns on the oxygen isotope ratio of tree rings in the Alpine region. J Geophys Res Atmos 117:D05118. https://doi.org/10.1029/2011JD016861
Saurer M, Spahni R, Frank DC, Joos F, Leuenberger M, Loader NJ et al (2014) Spatial variability and temporal trends in water-use efficiency of European forests. Glob Change Biol 20:3700–3712. https://doi.org/10.1111/gcb.12717
Schmidt H-L, Werner RA, Roßmann A (2001) ^{18}O Pattern and biosynthesis of natural plant products. Phytochemistry 58:9–32. https://doi.org/10.1016/S0031-9422(01)00017-6
Shu Y, Feng X, Posmentier ES, Sonder LJ, Faiia AM, Yakir D (2008) Isotopic studies of leaf water. Part 1: A physically based two-dimensional model for pine needles. Geochim Cosmochim Acta 72:5175–5188. https://doi.org/10.1016/j.gca.2008.05.062
Sidorova OV, Siegwolf RTW, Saurer M, Shashkin AV, Knorre AA, Prokushkin AS et al (2009) Do centennial tree-ring and stable isotope trends of Larix gmelinii (Rupr.) Rupr. indicate increasing water shortage in the Siberian north? Oecologia 161:825–835. https://doi.org/10.1007/s00442-009-1411-0
Sternberg LDSL, Deniro MJ, Savidge RA (1986) Oxygen isotope exchange between metabolites and water during biochemical reactions leading to cellulose synthesis. Plant Physiol 82:423–427. https://doi.org/10.1104/pp.82.2.423
Szejner P, Wright WE, Babst F, Belmecheri S, Trouet V, Leavitt SW et al (2016) Latitudinal gradients in tree ring stable carbon and oxygen isotopes reveal differential climate influences of the North American Monsoon System: intra-annual tree ring C and O isotopes. J Geophys Res Biogeosciences 121:1978–1991. https://doi.org/10.1002/2016JG003460
Treydte KS, Schleser GH, Helle G, Frank DC, Winiger M, Haug GH et al (2006) The twentieth century was the wettest period in northern Pakistan over the past millennium. Nature 440:1179–1182. https://doi.org/10.1038/nature04743
Treydte K, Frank D, Esper J, Andreu L, Bednarz Z, Berninger F et al (2007) Signal strength and climate calibration of a European tree-ring isotope network. Geophys Res Lett 34:L24302. https://doi.org/10.1029/2007GL031106
Treydte K, Boda S, Graf Pannatier E, Fonti P, Frank D, Ullrich B et al (2014) Seasonal transfer of oxygen isotopes from precipitation and

soil to the tree ring: source water versus needle water enrichment. New Phytol 202:772–783. https://doi.org/10.1111/nph.12741
van Bel AJE (2003) The phloem, a miracle of ingenuity. Plant Cell Environ 26:125–149
Vitali V, Klesse S, Weigt R, Treydte K, Frank D, Saurer M et al (2021) High-frequency stable isotope signals in uneven-aged forests as proxy for physiological responses to climate in Central Europe. Tree Physiol 00:1–17. https://doi.org/10.1093/treephys/tpab062
Watson E, Luckman BH (2002) The dendroclimatic signal in Douglas-fir and ponderosa pine tree-ring chronologies from the southern Canadian Cordillera. Can J for Res 32:1858–1874
West AG, Patrickson SJ, Ehleringer JR (2006) Water extraction times for plant and soil materials used in stable isotope analysis. Rapid Commun Mass Spectrom 20:1317–1321. https://doi.org/10.1002/rcm.2456
Wickham H (2016) ggplot2: Elegant graphics for data analysis. Springer-Verlag, New York
Williams AP, Cook ER, Smerdon JE, Cook BI, Abatzoglou JT, Bolles K et al (2020) Large contribution from anthropogenic warming to an emerging North American megadrought. Science 368:314–318. https://doi.org/10.1126/science.aaz9600
Wright WE, Leavitt SW (2006) Needle cell elongation and maturation timing derived from pine needle cellulose $\delta^{18}O$. Plant Cell Environ 29:1–14. https://doi.org/10.1111/j.1365-3040.2005.01394.x